IEEE Access
Multidisciplinary | Rapid Review | Open Access Journal

Received March 6, 2019, accepted May 27, 2019, date of publication June 10, 2019, date of current version July 3, 2019.

Digital Object Identifier 10.1109/ACCESS.2019.2921870

Universal Direct Tuner for Loop Control in Industry

ROBIN DE KEYSER[1], CRISTINA I. MURESAN[2], AND CLARA M. IONESCU[1,2,3], (Senior Member, IEEE)

[1]Research Lab on Dynamical Systems and Control, Faculty of Engineering and Architecture, Ghent University, 9052 Ghent, Belgium
[2]Department of Automatic Control, Technical University of Cluj-Napoca, 400114 Cluj-Napoca, Romania
[3]EEDT Core Lab on Decision and Control, Flanders Make Consortium, 9052 Ghent, Belgium

Corresponding author: Clara M. Ionescu (claramihaela.ionescu@ugent.be)

This work was supported in part by the Special Research Fund of Ghent University under Project MIMOPREC-STG020-18, and in part by the grant of the Romanian National Authority for Scientific Research and Innovation, CNCS/CCCDI-UEFISCDI, under Project PN-III-P1-1.1-TE-2016-1396 and Project TE 65/2018.

ABSTRACT This paper introduces a direct universal (automatic) tuner for basic loop control in industrial applications. The direct feature refers to the fact that a first-hand model, such as a step response first-order plus dead time approximation, is not required. Instead, a point in the frequency domain and the corresponding slope of the loop frequency response is identified by single test suitable for industrial applications. The proposed method has been shown to overcome pitfalls found in other (automatic) tuning methods and has been validated in a wide range of common and exotic processes in simulation and experimental conditions. The method is very robust to noise, an important feature for real life industrial applications. Comparison is performed with other well-known methods, such as approximate M-constrained integral gain optimization (AMIGO) and Skogestad internal model controller (SIMC), which are indirect methods, i.e., they are based on a first-hand approximation of step response data. The results indicate great similarity between the results, whereas the direct method has the advantage of skipping this intermediate step of identification. The control structure is the most commonly used in industry, i.e., proportional–integral–derivative (PID) type. As the derivative action is often not used in industry due to its difficult choice, in the proposed method, we use a direct relation between the integral and derivative gains. This enables the user to have in the tuning structure the advantages of the derivative action, therefore much improving the potential of good performance in real life control applications.

INDEX TERMS Frequency response, noise measurement, control systems, robustness, tuning.

I. INTRODUCTION

Industry often relies on simple tests during process operation to detect changes in process dynamics and adapt control parameters to maintain the desired closed loop performance specifications. Often, the test is what is known as a 'bump' test, or, in control community known as a 'step response' test [1], [2]. Recent industry-academia gatherings have tackled the problem of Industry 4.0 requirements and identified a set of bottlenecks. The Linnaeus Center for Control of Complex Engineering Systems at Lund University, Sweden, hosted the workshop on Process Control [3], in collaboration with the Process Control Centre at Lund University, a reference address for automatic tuning control. It was held at Pufendorf Institute in Lund, 26-28 September 2016, and attended by 60 international persons, organizers included. From the three discussion groups i) current challenges, ii) industry meets academia and iii) future visions, the following problems emerged, here is a simplified extract of the meeting book report.

- Many PID (proportional-integral-derivative) controllers are in manual or have default settings, but most of the participants seemed to be unaware or unworried about the situation. When the PID controllers are used at the bottom layer under MPC (model predictive control), they are often tuned when MPC is commissioned, but they are unfortunately not maintained tuned; according to industry reports, controllers lose 60% of their performance after the first 6 months [4].

The associate editor coordinating the review of this manuscript and approving it for publication was Shuangqing Wei.

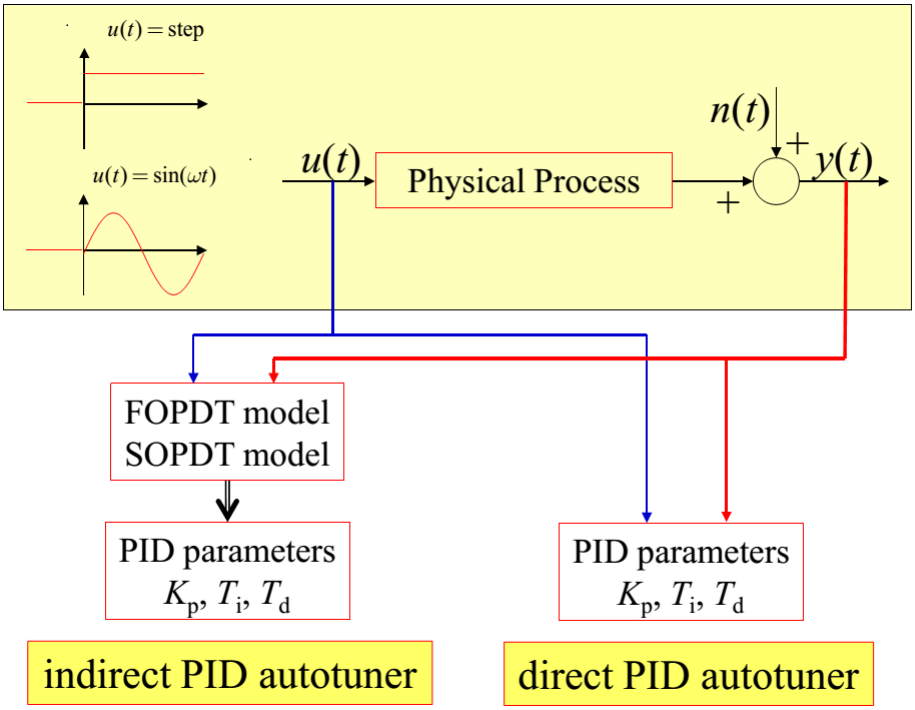

FIGURE 1. Graphical abstract of the tuning schemes for controller parameters extracted from process information.

- Related to the use of big data, it is hard to find sequences of data useful for identification and modeling, since most of it is closed-loop data, meaning that causality may be reversed. One solution is to look when loops are in manual mode, or when setpoint changes occur.
- The technology used in automation software is old, often from the 60s and 70s; the systems are clumsy and hard to use. Large overhead in terms of engineering hours are needed to execute simple tasks as replacing a sensor. Compared to other systems (smart phones for example), there is a huge technological gap, which is widening further.
- Monitoring is an essential element in the long-term (optimal) functioning of the plant.
- Wireless will become the default communication mechanism.

Secondly considered were latest annual IEEE academia-industry conferences on Emerging Technologies and Factory Automation, in September 2017 and 2018 [5]. Similar messages emerged from the academia-industry discussion panels during both meetings. Finally, another event was perused: the 3rd IFAC International Conference on Advances in Proportional-Integral-Derivative Control (PID18), held in Ghent, Belgium, 9-11 May 2018 [6]. Once again, the academia and industry were present and involved in discussions, where similar messages as above mentioned emerged.

In a recent review of the most common issues in industry indicated the use of PID control and MPC as the two most encountered in industry [7]. The essential problem remains undoubtedly the tuning of lower loops as a pre-requisite for good performance achieved with higher loop / supervisory loop control. It is a mistake to put higher loop control in charge of dealing with poor performance stemming from poor tuning of lower loop control levels in the process hierarchy. In this context, (automatic) tuning from ongoing process operation data is the key to success.

This paper proposes a solution to this problem and positions the work in the industry-demand framework. The paper is structured as follows: first, some preliminaries are given as to introduce the rationale and the indirect controller tuning methods used for comparison. The third section describes the methodology behind this universal tuner. Results in simulation are summarized on most representative processes in the fourth section, followed by the experimental validation, and implementation issues. A conclusion section summarizes the main outcome of this work and points to new directions.

II. PRELIMINARIES

A. STEP RESPONSE - INDIRECT TUNING METHODS

The indirect tuning methods are those which prior to control parameter tuning require identification of basic step response data to first order plus dead time (FOPDT) or second order plus dead time (SOPDT) [8], [9]. By contrast, direct methods skip this identification step. Fig. 1 provides this concept in graphical form.

Identification for the purpose of control is a demanding step in the process of model development of dynamical

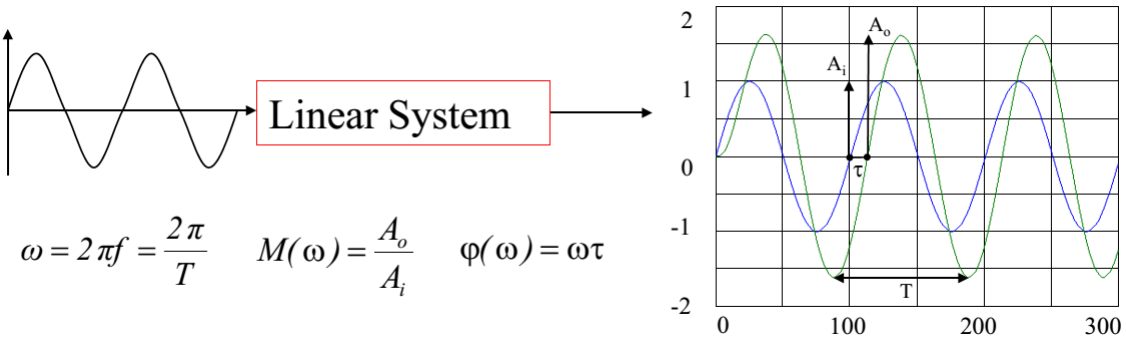

FIGURE 2. Schematic identification of modulus and phase in a single frequency point for linear systems.

systems. Latest reviews for industrial relevance indicate that system identification plays an important role in practice [10]. Identification methods vary in terms of complexity, depending on the scope of the target model usage. Methods for system identification are available in both time- and frequency-domains. Most commonly used in industry are the step test response data, relay test data and sinusoid test data. Suitable methods for industrial process control are event-based algorithms, where basic identification plays an important role before tuning controller parameters [11]–[13].

Relay based methods have been one of the first used to automatic tuning of PID-type controllers [14]–[16]. However, they also have been revised for identification of process model from data [17], [18] as to improve their performance.

Some example of methods using step response data are summarized in [19]–[21] and [22]. Of these, most commonly used are AMIGO (Approximate M-constrained Integral Gain Optimization) [14] and SIMC (Skogestad Internal Model Controller) [23].

The AMIGO method uses a FOPDT process approximation of the form:

$$\frac{Ke^{-\tau s}}{1+Ts} \tag{1}$$

with K the gain, τ the time delay and T the time constant of the approximation to step response data of the process. It then uses a parallel PID configuration with the tuning rules:

$$\begin{aligned} K_p &= \frac{1}{K}\left(0.2 + 0.45\frac{T}{\tau}\right) \\ T_i &= \tau\left(\frac{0.4\tau + 0.8T}{\tau + 0.1T}\right) \\ T_d &= \tau\left(\frac{0.5T}{0.3\tau + T}\right) \end{aligned} \tag{2}$$

The SIMC method uses a SOPDT process approximation of the form:

$$\frac{Ke^{-\tau s}}{(1+T_1 s)(1+T_2 s)} \tag{3}$$

with K the gain, τ the time delay and $T_1 > T_2$ the time constants of the approximation to step response data of the process. It then uses a series PID configuration with the tuning rules:

$$\begin{aligned} K_p &= \frac{T_1}{2K\tau} \\ T_i &= min(T_1, 8\tau) \\ T_d &= T_2 \end{aligned} \tag{4}$$

B. FREQUENCY RESPONSE TUNING METHODS

Frequency response function (FRF) of a dynamical system is a measure of the modulus and phase of the output signal as a function of an input frequency, relative to the input signal applied to the system. FRF allows one to determine approximate models for the process to be controlled. To appropriately characterize the process dynamics in a given frequency interval, the gathered information must cover the modulus, phase and their corresponding slopes with respect to frequency. Classical methods for estimating FRF are based on input and output data followed by Fast Fourier Transform (FFT). These procedures usually require multiple or persistent exciting tests with input signals of various frequencies, so that the frequency response can be estimated over the required frequency range [24].

For linear systems, a sinusoidal input of amplitude A_i and frequency f yields a sinusoidal output of same frequency as the input, shifted in time τ and with different amplitude A_o and period T. The modulus is given by the ratio of output amplitude and the input amplitude for the input frequency tested in the system. The phase is the time shift between the input-output signals, as summarized in Fig. 2.

When the FRF is required around certain frequency, it is pragmatic to reduce the number of unnecessary experiments, complexity and time-to-deliver by using an efficient and reliable algorithm. The result should be the modulus, the phase and the corresponding frequency response slope in/around a specified frequency [25], [26].

A large number of applications that require the frequency response slope justify the necessity for developing such an algorithm. For instance, in [16] a relay-based method is used, with the identification method being automated and thus useful for autotuning applications. The frequency response

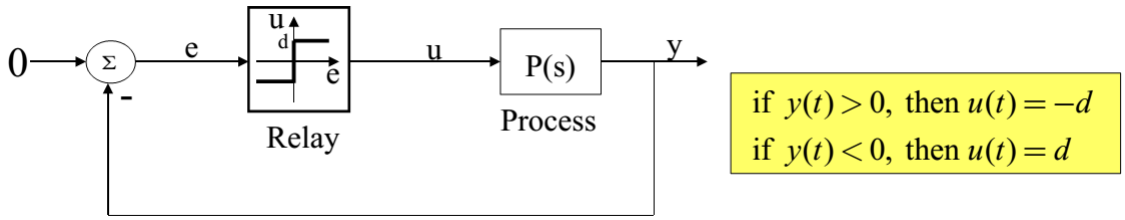

FIGURE 3. The scheme of the relay feedback test.

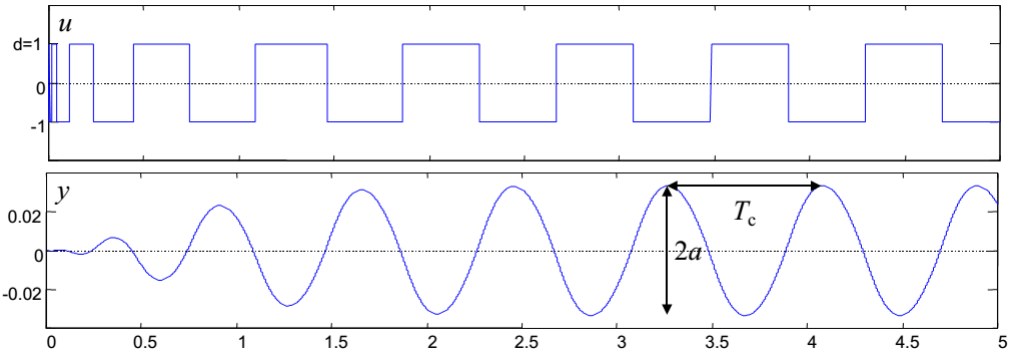

FIGURE 4. Input-output representation of a relay feedback test and essential information gathered from this test.

slope is considered to be a measure of the process complexity and it can be used to determine the relative degree of a process. The slope of the frequency response modulus is estimated at the gain crossover frequency. This information is used as a part of the initialization procedure for the tuning of an adaptive controller. Computation of the frequency response slope has also found applications in the estimation of non-stationary sinusoidal parameters for sinusoids with linear AM/FM modulation [27]. Here, an enhanced algorithm for frequency domain demodulation of spectral peaks is proposed and it is used to obtain an approximate maximum likelihood estimate of the frequency slope, as well as an estimate of the amplitude, phase and frequency parameter with significantly reduced bias.

In [28] Bode's integrals are used to approximate frequency response slope of a system at a given frequency, without any model of the plant. This information is then used to design a PID controller for slope adjustment of the Nyquist diagram and improve the closed-loop performance. Additionally, the frequency response slope is also employed in the estimation of the gradient and the Hessian of a frequency criterion, defined as the sum of squared errors between the desired and measured gain margin, phase margin and crossover frequency, in an iterative PID controller tuning method.

Emerging industrial controllers of higher degree of freedom are fractional order controllers [7], [29], [30]. The phase slope of the FRF has been used in the design of fractional order PD/PI controller based on an auto-tuning method that requires knowledge of the process modulus, phase and phase slope at an imposed gain crossover frequency [31].

A popular direct PID tuner is based on relay feedback test, with amplitude d as depicted in Fig. 3, with the result given in Fig. 4. This test identifies the modulus at the critical frequency, i.e. the point of intersection with the negative real axis in the Nyquist plane. The period of oscillation T_c, and the amplitude of the oscillation a are the used to tune the PID-type control parameters. The most known method is the Ziegler Nichols, and the later revised Ultimate Cycle Method, with tuning rules:

$$\begin{aligned} K_c &= \frac{4d}{\pi a} \\ K_p &= 0.6K_c \\ T_i &= 0.5T_c \\ T_d &= 0.125T_c \end{aligned} \tag{5}$$

This commonly used in industry tuner provides a standard robustness of 0.5 (on a range from 0 to 1) in the Nyquist plane.

A method based on the same test was proposed in [32], with one degree of freedom, i.e. to specify the desired phase margin of the loop. Hence, the user may alter the robustness provided by the tuner, and vary its value according to the process dynamics. From the same relay feedback test and specified phase margin (PM) value (commonly selected between 40-75 degrees), the tuning rules are:

$$\begin{aligned} K_c &= \frac{4d}{\pi a} \\ K_p &= K_c \cos PM \\ T_i &= T_c \frac{1 + \sin PM}{\pi \cos PM} \\ T_d &= 0.25T_i \end{aligned} \tag{6}$$

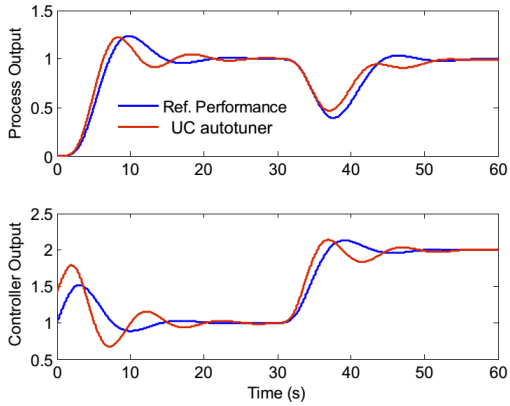

FIGURE 5. Result for the high order process.

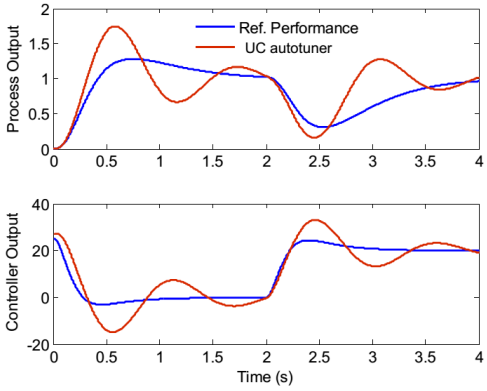

FIGURE 6. Result for the integrating process.

Notice the relation $T_i = 4T_d$; this is a commonly used choice to simplify the tuning procedure; it assumes two identical real zeros in the PID controller.

C. EXAMPLES AND COUNTER EXAMPLES

An example of a process which is not obvious to control with a PID-type controller is a high order process as in

$$P_1(s) = \frac{1}{(s+1)^6} \tag{7}$$

The result of the ultimate cycle (UC) method autotuner is given in Fig. 5. The reference performance for comparison has been done using the process model and a model based controller tuning method (e.g. can be any method of user's choice, CAD packages, root locus, etc). It can be observed that the autotuner performs equally well as the model based tuner.

Now, let us consider the following commonly used in practice process model (i.e. any positioning system):

$$P_2(s) = \frac{32}{s(s+3)(s+21)} \tag{8}$$

and the result of the UC tuner is given in Fig. 6, with less good performance against the model based tuner. The Nyquist diagram of the corresponding loop is given in Fig. 7, where is

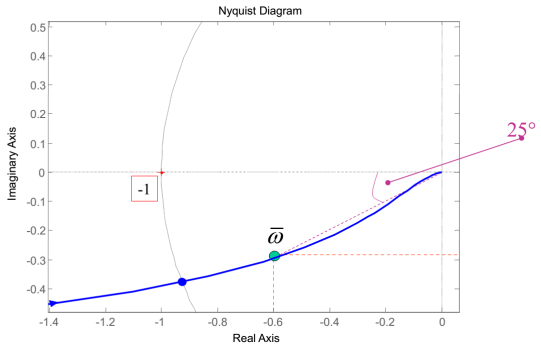

FIGURE 7. Insight into the Nyquist diagram of the loop frequency response.

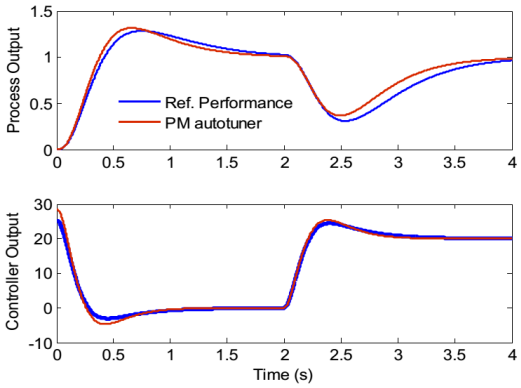

FIGURE 8. Adapted specification delivers good results for the integrating process.

can be observed a mere phase margin of 25 degrees is ensured, due to the existence of the integrator (i.e. lower frequencies effect with a phase of -270 degrees).

Alternatively, if the phase margin method is used with a specified value of 50 degrees, the result improves to a comparable performance in closed loop as the model based tuner - as illustrated in Fig. 8.

Let us again consider a commonly used process in industry (i.e. delay dominant system):

$$P_3(s) = \frac{100}{(1+5s)(1+10s)} e^{-25s} \tag{9}$$

and tune a PID controller with the phase margin specified at 70 degrees (high robustness). The result is depicted in Fig. 9. As observed, the PM tuner delivers unstable loop results for this kind of process, while the model based tuner gives satisfactory results. The insight in the PM tuner failure is that due to the high values of time delay, the loop modulus increases slightly as the loop angle decreases at high frequencies, resulting in the fact that the loop goes beyond the critical point (0,−1), i.e. unstable result.

D. PRELIMINARY CONCLUSIONS

As a summarizing thought, not only the choice of the FR point, but also the slope of the FR loop is important for the closed loop performance.

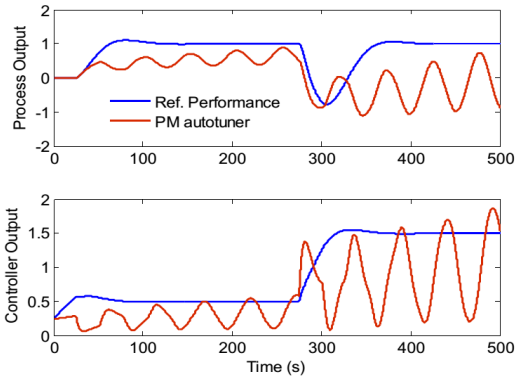

FIGURE 9. Result for the time delay process.

A direct tuner is a very attractive option for PID control from practical point of view, as it does not require apriori identification. A plethora of papers and books have presented relay feedback PID tuning methods as direct methods for tuning controller parameters. However, as shown here, it is not universally successful as the user still has to make some choices depending on the type of process at hand. Yet another plethora of other PID (automatic) tuning methods have been published with excellent results, successful in practice.

From the above insight, it follows that specifying a point in frequency domain does not suffice for the loop to be guaranteed stable. Additional specifications for the loop slope towards high frequencies is equally important. This can be achieved by specifying a forbidden zone as a circle, and imposing the loop is tangent to this circle. It may be an optimization procedure including other specifications like gain margin, phase margin, etc.

The next section introduces the concept and method for a direct tuning method which counteracts the pitfalls of the previous examples.

III. PROPOSED METHODOLOGY

A. THEORETICAL PRINCIPLES FOR PROCESS FR SLOPE CALCULATION

To determine the frequency response (modulus and phase) of any stable process at a specific frequency $\bar{\omega}$, a sinusoidal input signal $u(t) = A_u \sin(\bar{\omega})$ is applied to the process as in Fig. 10. The FR of the process is then

$$P(j\bar{\omega}) = \frac{A_y}{A_u} e^{j\phi_y} = M e^{j\phi} \tag{10}$$

The process derivative is used to determine the output signal $\bar{y}(t)$:

$$\bar{Y}(s) = \frac{dP(s)}{ds} U(s) \tag{11}$$

and the corresponding frequency response in

$$\frac{dP(j\omega)}{d(j\omega)}\Big|_{\omega=\bar{\omega}} = \frac{A_{\bar{y}}}{A_u} e^{j\phi_{\bar{y}}} = \bar{M} e^{j\bar{\phi}} \tag{12}$$

Theorem 1: If the process input is $u(t)$, then the output $\bar{y}(t)$ of the process derivative is given by $\bar{y}(t) = x(t) - t \cdot y(t)$, with $x(t)$ the process output.

Proof is given in Appendix.

The FR of the process can be separated in a real $R(\bar{\omega})$ and an imaginary $I(\bar{\omega})$ part from (10). The derivative can also be separated in a real and imaginary part from (12) as in

$$\frac{dP(j\omega)}{d(j\omega)}\Big|_{\omega=\bar{\omega}} = \frac{dR(\omega)}{d\omega}\Big|_{\omega=\bar{\omega}} + j\frac{dI(\omega)}{d\omega}\Big|_{\omega=\bar{\omega}} \tag{13}$$

Having the real and imaginary parts available as input, one may calculate the modulus derivative as in

$$\frac{dM(\omega)}{d\omega}\Big|_{\omega=\bar{\omega}} = \frac{1}{M}\left(R(\bar{\omega})\frac{dR(\omega)}{d\omega}\Big|_{\omega=\bar{\omega}} + I(\bar{\omega})\frac{dI(\omega)}{d\omega}\Big|_{\omega=\bar{\omega}}\right) \tag{14}$$

and the phase derivative as in

$$\frac{d\phi(\omega)}{d\omega}\Big|_{\omega=\bar{\omega}} = \frac{1}{M^2}\left(R(\bar{\omega})\frac{dI(\omega)}{d\omega}\Big|_{\omega=\bar{\omega}} - I(\bar{\omega})\frac{dR(\omega)}{d\omega}\Big|_{\omega=\bar{\omega}}\right) \tag{15}$$

This method is useful in ideal situations, simulation studies and in processes without noise. In practice however, processes and signals in general are affected by stochastic disturbances and noise that could potentially alter the final result. The following example illustrates this situation and justifies the need to robustify the proposed method. Consider the mass-spring-damper system from Fig. 11. Mass-spring-dampers systems are generally used to study behavior of the yarn in weaving machines, active suspension system, trains or chain of cars on highways, tall buildings, airplane wings, etc. Applying a sine-test signal of frequency 33.4 rad/s, the output signal and its derivative are obtained as indicated in Fig. 12. Clearly, the measured output signal is corrupted with stochastic disturbances.

The scheme from Fig. 10 assumes unbounded signals $x(t)$ and $t*y(t)$, while their difference $\bar{y}(t)$ remains bounded. However, if the signal $y(t)$ contains other components than a pure sine, they are amplified by the filter, resulted in unbounded signal $\bar{y}(t)$.

B. ROBUST CALCULATION OF THE PROCESS FR SLOPE CALCULATION

A realistic form of the process output is given by

$$y(t) = A_y \sin(\bar{\omega}t + \phi_y) + b + n(t) \tag{16}$$

with zero average stochastic disturbance $n(t)$ and non-zero bias term b for an integrative process, otherwise $b = 0$. Using standard transfer function analyser principles, problems of non-linear distortion and noise corruption are overcome if the measured output $y(t)$ is first multiplied by sine and cosine respectively of the input frequency, followed by integration over the measurement period $T_m = k\frac{2\pi}{\bar{\omega}}$. After sufficient measurement time, only the term directly proportional to

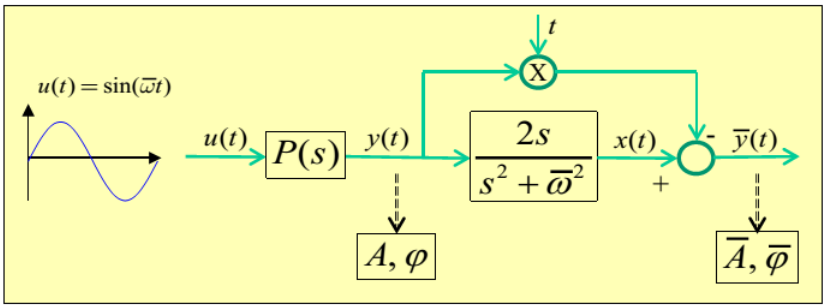

FIGURE 10. Basic scheme for calculating the slope of the frequency response of the process from a single sine test.

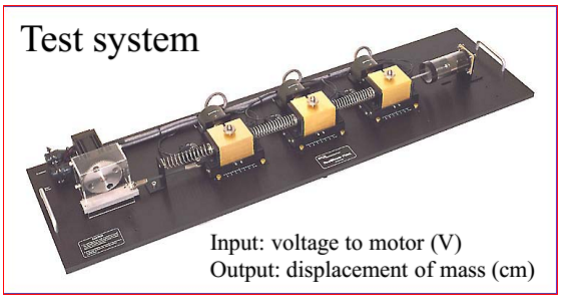

FIGURE 11. Mass-spring-damper system – experimental unit; the position of the second mass (in the middle position) is the one to be measured as output. The input is the linear motor on the far left of the setup. The damper on the far right of the setup is not connected, in order to provide poor damping in system dynamics.

measurement time remains significant, e.g. the signal multiplied with the sine function becomes:

$$y_s = 0.5T_m A_y \cos\phi_y \tag{17}$$

and similarly for the signal multiplied with the cosine function. Combining them leads to the relation

$$\begin{aligned} y_c - jy_s &= \int_0^{T_m} y(t)(\cos(\bar{\omega}t) - j\sin(\bar{\omega}t))dt \\ &= \int_0^{T_m} y(t)e^{-j\bar{\omega}t}dt \end{aligned} \tag{18}$$

whereas the last term can be calculated via discrete Fourier Transform as in

$$\int_0^{T_m} y(t)e^{-j\bar{\omega}t}dt = T_s \sum_0^{N-1} y(kT_s)e^{-j\bar{\omega}kT_s} \tag{19}$$

with the sampling period T_s adequately chosen such that $T_m = NT_s$, with N the total number of measured samples. We can also write

$$y_c - jy_s = -j0.5T_m A_y e^{j\phi_y} \tag{20}$$

from where we can summarize the forms of amplitude and phase of the output signal are given by

$$A_y e^{j\phi_y} = \frac{2j}{N}\sum_0^{N-1} y(kT_s)e^{-j\bar{\omega}kT_s} \tag{21}$$

For the calculation of the slope of the process, we consider Fig. 13 where $y_{TR}(t)$ is the transient part and $y_{SS}(t)$ is the steady state part of the output signal $y(t)$, assuming the transient part going to zero (or to a constant value for integrating systems).

The steady-state component can be defined as

$$y_{ss}(t) = A_y \sin(\bar{\omega}t + \phi_y) = S\sin(\bar{\omega}t) + C\cos(\bar{\omega}t) \tag{22}$$

where $S = A_y\cos(\phi_y)$ and $C = A_y\sin(\phi_y)$. Laplace transform gives

$$Y_{SS}(s) = \frac{S\bar{\omega}}{s^2+\bar{\omega}^2} + \frac{Cs}{s^2+\bar{\omega}^2} = \frac{S\bar{\omega}+Cs}{s^2+\bar{\omega}^2} \tag{23}$$

with the derivative given by

$$\frac{dY_{SS}(s)}{ds} = \frac{C}{s^2+\bar{\omega}^2} - \frac{2s}{s^2+\bar{\omega}^2}Y_{SS}(s) \tag{24}$$

and its inverse Laplace transform is

$$-t\cdot y_{ss}(t) = \frac{A_y\sin(\phi_y)}{\bar{\omega}}\sin(\bar{\omega}t) - L^{-1}\{\frac{2s}{s^2+\bar{\omega}^2}Y_{SS}(s)\} \tag{25}$$

This result suggest to replace Fig. 13 by the new scheme in Fig. 14.

The Laplace of the signal $x(t)$ can now be computed as

$$\bar{X}(s) = \frac{2s}{s^2+\bar{\omega}^2}Y_{TR}(s)\frac{\bar{\omega}}{s^2+\bar{\omega}^2} \tag{26}$$

with

$$\bar{x}(t) = L^{-1}\{\frac{2s}{\bar{\omega}}Y_{TR}(s)\}\sin(\bar{\omega}t) \tag{27}$$

As the component $t\cdot y_{TR}(t)$ does not influence the steady-state oscillation in $\bar{y}(t)$ or $\bar{x}(t)$, this is then the final form.

For the special case of integrating systems, the transient signal $y_{TR}(t)$ converges to a constant value y_c. In this case, the DFT of $|y_{TR}(t) - y_c|$ is firstly calculated and afterwards corrected with the FT of a step signal with amplitude y_c. In other words, a scaling factor of $y_c/(j\bar{\omega})$ should be added.

The FR slope of the process *algorithm* is summarized below:

- perform a sine test
- analyze steady-state oscillation to determine amplitude A_y and phase ϕ_y

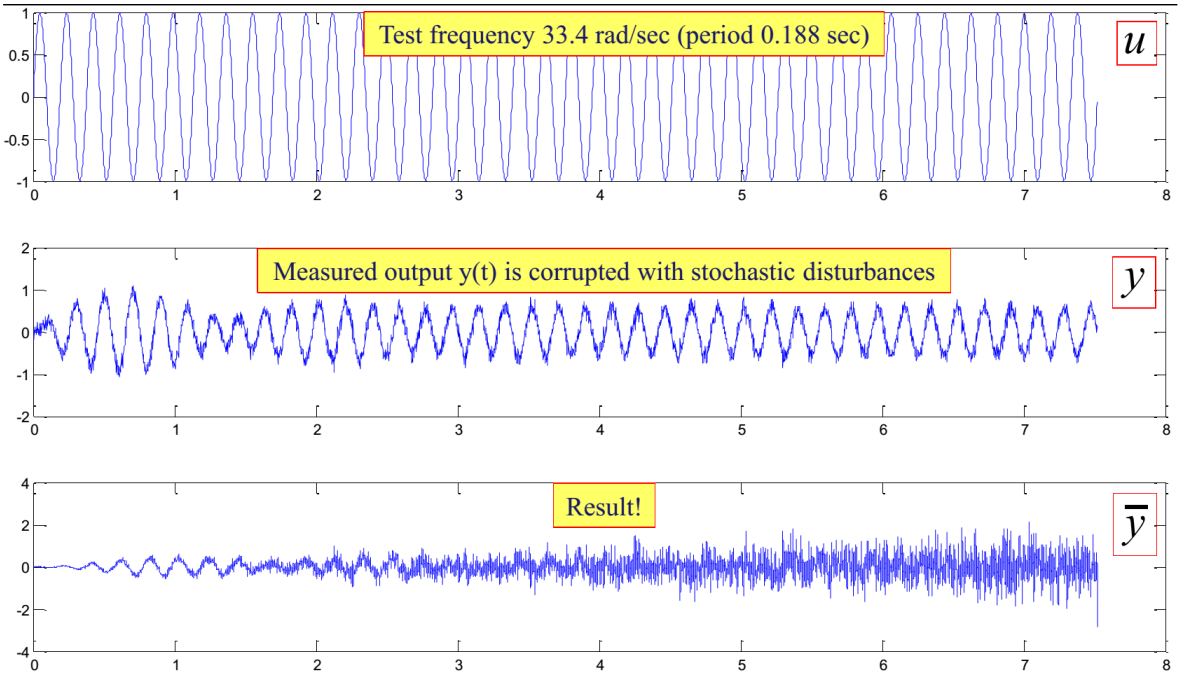

FIGURE 12. Sine-test results on a real mass-spring-damper system; one may observe the result does not converge to a useful value due to noise and disturbances.

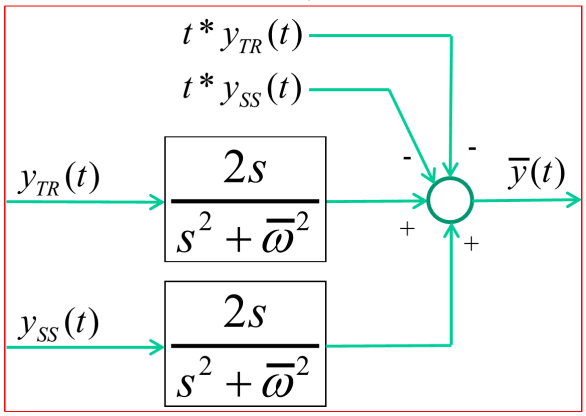

FIGURE 13. Preliminary solution to the robust scheme for determining the frequency response slope.

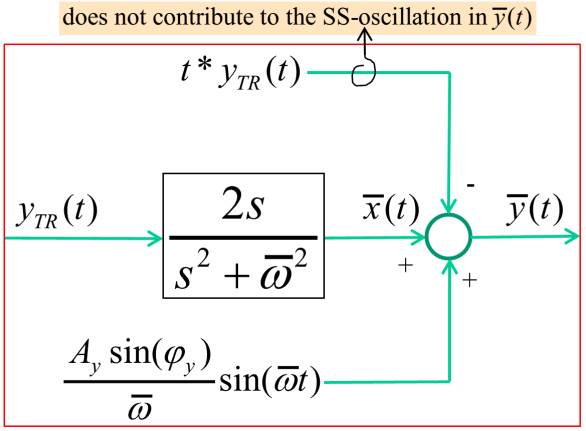

FIGURE 14. Final solution to the robust scheme for determining the frequency response slope.

- calculate transient part as $y_{TR}(t) = y(t) - y_{ss}(t)$, with $y_{ss}(t) = A_y \sin(\bar{\omega}t + \phi_y)$
- calculate the complex number

$$A_{\bar{y}} e^{j\phi_{\bar{y}}} = 2jT_s \sum_{k=0}^{N-1} y_{TR}(kT_s) e^{-j\bar{\omega}kT_s} + \frac{A_y \sin(\phi_y)}{\bar{\omega}}$$

- calculate the FR of the process and the FR slope at the test frequency $\bar{\omega}$:

$$P(j\bar{\omega}) = \frac{A_y}{A_u} e^{j\phi_y}$$

$$\text{and } \frac{dP(j\omega)}{d(j\omega)}\Big|_{\omega=\bar{\omega}} = j\frac{A_{\bar{y}}}{A_u} e^{j\phi_{\bar{y}}}$$

This concludes the slope calculation of the process from a single sine test.

C. CALCULATION OF THE LOOP FR SLOPE

The loop frequency response contains the process and controller FRF for the known frequency. For a known controller $C(s)$, the values for $C(j\bar{\omega})$ and $\frac{dC(j\omega)}{d\omega}\big|_{\bar{\omega}}$ can be easily obtained. The process values for $P(j\bar{\omega})$ and $\frac{dP(j\omega)}{d\omega}\big|_{\bar{\omega}}$ are obtained from the sine test described in previous subsections. The loop FRF is given then by:

$$\frac{dL(j\omega)}{d\omega} = P(j\omega)\frac{dC(j\omega)}{d\omega} + C(j\omega)\frac{dP(j\omega)}{d\omega} \tag{28}$$

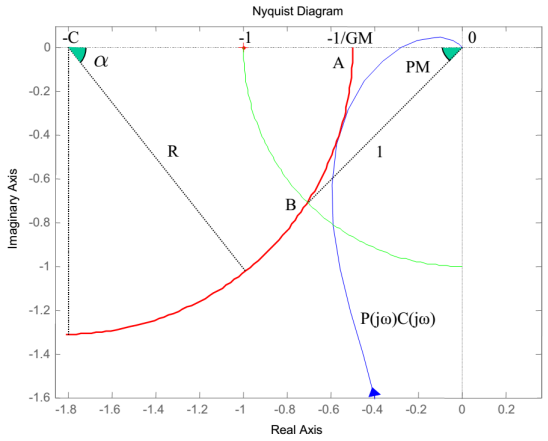

FIGURE 15. Nyquist diagram of loop FRF and circle of forbidden zone for tuning controller parameters.

D. CALCULATION OF THE CIRCLE SLOPE

The user defined circle as the forbidden zone of the loop FRF, is defined by the relation

$$(Re + C)^2 + Im^2 = R^2 \tag{29}$$

and goes through: point A - defined as the gain margin GM and point B - defined as the phase margin PM. Fig. 15 provides essential information in the Nyquist plane used to optimize the angle α necessary in the tuning of the controller parameters.

In Fig. 15, point A is given by relation $(-1/GM + C)^2 = R^2$ and point B is given by relation $(-\cos PM + C)^2 + (-\sin PM)^2 = R^2$. It follows equality $C^2 - 2\cos PM * C + 1 = C^2 - 2C/GM + 1/GM^2$. From here one can extract the value of the circle center and circle radius as in

$$C = \frac{GM^2 - 1}{2GM(GM\cos PM - 1)}$$
$$R = C - \frac{1}{GM} \tag{30}$$

The complex number of the positions on the circle are given by $Re = -C + R\cos\alpha$ and $Im = -R\sin\alpha$. The angle of the slope is given by $\alpha_C = 90^o - \alpha$.

It follows an optimization procedure for $0 \leq \alpha \leq \alpha_{max}$ such that $|\alpha_L - \alpha_C|$ is minimized. This then delivers the information for the last step in the tuner procedure summarize din the next subsection.

E. DIRECT TUNER PROCEDURE

Having all the information at hand from previous subsections, the direct tuner algorithm consists of several steps summarized hereafter:

- select a test frequency $\bar{\omega}$, e.g. gain cross over frequency ω_c; other frequencies may be chosen in the 3rd quadrant
- perform a sine-test on the process $P(s)$; the result is then the frequency response information at that test-frequency $P(j\bar{\omega})$ and the slope $\frac{dP(j\omega)}{d\omega}\big|_{\bar{\omega}}$
- define a forbidden region around the -1 point in the Nyquist plane as a circle

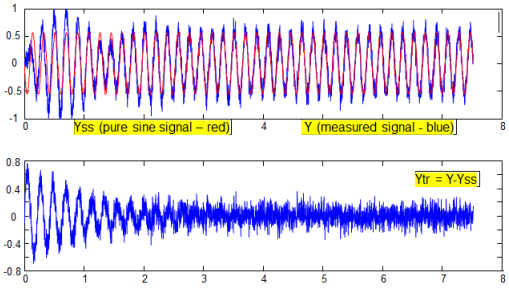

FIGURE 16. Signals used in the MSD setup for slope calculation.

- for each point on the circle: calculate a PID controller C(s) such that the loop frequency response $L(j\omega) = P(j\omega)C(j\omega)$ goes through a single point on this circle (see next step)
- find the point on the circle for which the loop frequency response touches the circle (kisses the circle / Kiss Circle (KC) method), i.e the difference between the slope of the circle and the slope of the frequency response is minimum
- select the PID parameters from the last step

In Appendix the reader may consider further support in implementing the procedure in practice.

IV. RESULTS

A. SIMULATION AND EXPERIMENTAL VALIDATION OF THE SLOPE CALCULATION

In order to indicate the feasibility of the slope calculation for systems with noise and transients in the output signal, we reiterate the experimental validation on the mass-spring-damper system. For the purpose of validation, extensive identification led to the following process transfer function

$$P_{MSD}(s) = \frac{28340}{s^3 + 173.9s^2 + 1282s + 145600} \tag{31}$$

from which the critical frequency is $\bar{\omega} = 33.4$ rad/s, with the process value $P(j\bar{\omega}) = -0.578 - 0.0644j$ and its derivative $\frac{dP(j\omega)}{d(j\omega)}\big|_{\omega-\bar{\omega}} = 0.130 + 0.056j$. It follows the modulus and phase are $M(\bar{\omega}) = 0.581$ and $\phi(\bar{\omega}) = -173^o$, respectively. The slopes of the FRF modulus and phase are $\frac{d20logM(\omega)}{dlog(\omega)}\big|_{\omega=\bar{\omega}} = -155$ dB/dec and $\frac{d\phi(\omega)}{dlog(\omega)}\big|_{\omega=\bar{\omega}} = -207^o$/dec.

From the experimental test with the sine input, it follows the critical frequency $\bar{\omega} = 33.4$ rad/s, the FRF of process and its derivative are $-0.561 - 0.0264j$ and $0.131 + 0.032j$, respectively. The corresponding modulus is 0.562 and phase -177^o. The slopes of the FRF for modulus and phase are -157 dB/dec and -204^o/dec, respectively.

Hence, it can be concluded that the experimental values correspond well with the theoretical values for the system. Fig. 16 depicts the signals used to compute the slopes as detailed in this paper.

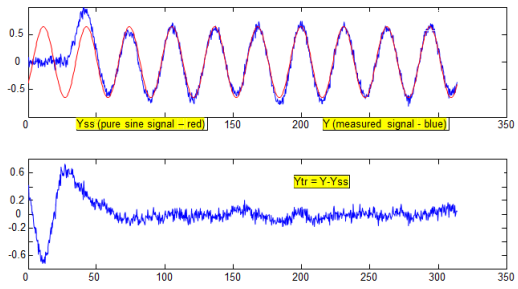

FIGURE 17. Signals used for the slope calculation for the delay dominant process.

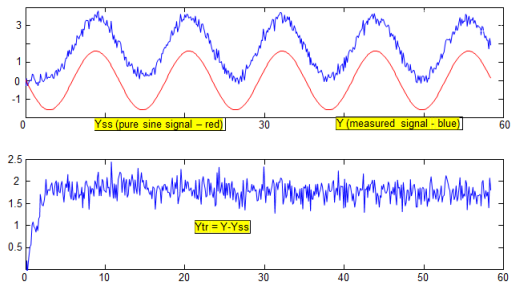

FIGURE 18. Signals used for slope calculation for the integrating process.

Another example for calculus of the slope is a time delay dominant system:

$$\frac{2e^{-25s}}{(1+5s)(1+10s)} \tag{32}$$

where noise has been added to mimic a real situation. The signals used to calculate the slope are given in Fig. 17, and again, a very good validation has been obtained.

Finally, an integrating system has been tested:

$$\frac{e^{-2s}}{s(1+s)} \tag{33}$$

with added noise and signals given in Fig. 18. This is particularly challenging as it contains both integrator and a considerable time delay value. The theoretical and experimental results of the proposed slope calculation method are again in agreement.

Other processes have been analyzed in simulation and in experimental setups. For instance, the slope calculation has been used in a mechatronic application of an industrial robot arm control as described in [34], [35]. Prior versions of slope calculation have been discussed in vibration systems control [36], in a multivariable nonlinear benchmark process [38] and in extensive simulation processes in [37].

B. SIMULATION AND EXPERIMENTAL VALIDATION OF THE UNIVERSAL TUNER

The method for the universal tuner parameter calculation using the FRF and slope calculation method has been extensively tested in simulation, with successful results on a

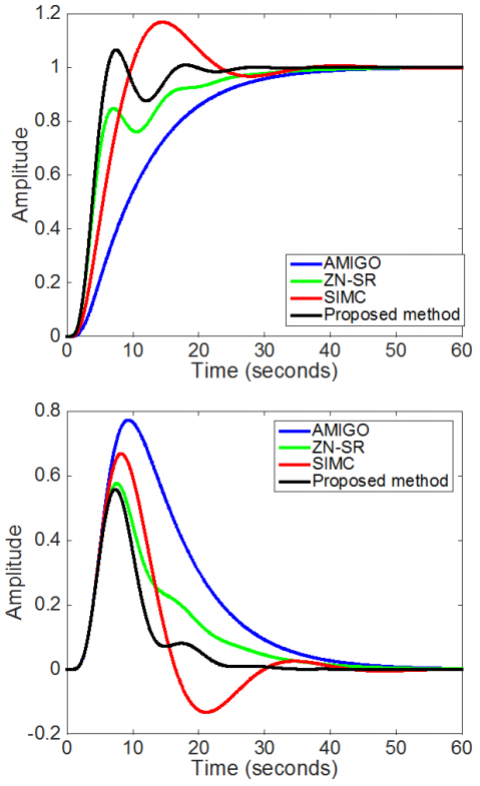

FIGURE 19. Comparison for the high order process.

plethora of type of processes. These processes with the specifications of gain margin GM = 2 dB, phase margin PM = 45 degrees, include:

$$\begin{gathered}
\frac{1}{(s+1)^6} \\
\frac{e^{-s}}{s(1+s)} \\
\frac{2}{(1+10s)(1+5s)(1+2s)} \\
\frac{(1-0.2s)e^{-0.1s}}{(s+1)^2} \\
\frac{498}{s(s^2+1.8s+36} \\
\frac{1.75(1-3s)(1-5s)e^{-1.25s}}{(1+10s)(1+4s)^2} \\
\frac{(s+6)^2}{s(s+1)^2(s+36)} \\
\frac{e^{-s}}{s(s+1)^3}
\end{gathered} \tag{34}$$

The full details on these processes and controller parameters can be found in [33]. From these, a selection is made and compared here against the ultimate gain method and the two tuners presented in the beginning of the paper: AMIGO and SIMC.

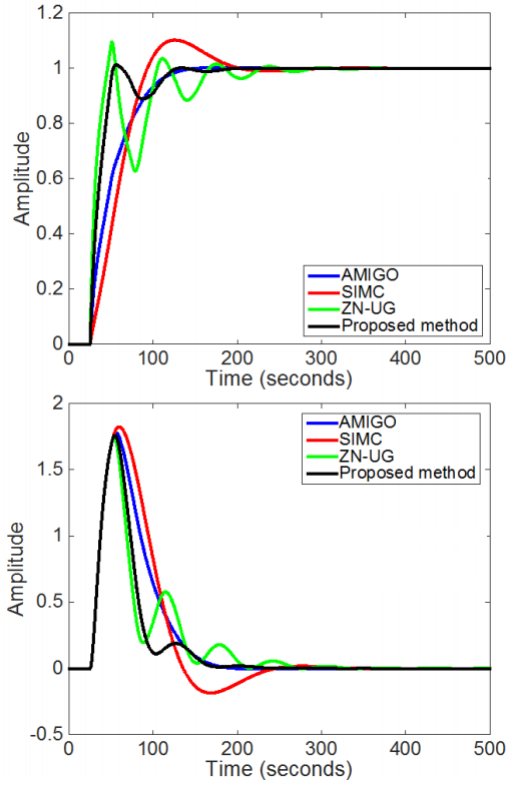

FIGURE 20. Comparison for the delay dominant process.

The high order process

$$\frac{1}{(s+1)^6} \tag{35}$$

with the universal tuner gives the reference tracking and load disturbance rejection from Fig. 19.

The dominant time delay process

$$\frac{0.04e^{-25s}}{(s+0.2)(s+0.1)} \tag{36}$$

with the universal tuner gives the reference tracking and load disturbance rejection from Fig. 20.

Finally, a nonlinear 6th order process is assembled with three Quanser modules of water tanks, as depicted in Fig. 21. The water is pumped from the water reservoir V_{p1}, V_{p2}, V_{p3} and entered the first tank (on the far left, upper tank L_1)), following in series the tanks, with the purpose to regulate the water level in the last tank (on the far right, lower tank L_6). A disturbance V is implemented by opening and closing the valve in the middle module.

From the step response, the AMIGO and SIMC process approximations necessary for the controller tuning are

$$\begin{aligned} FOPDT &: \frac{0.82e^{-30s}}{1+38s} \\ SOPDT &: \frac{0.82e^{-22s}}{(1+24s)(1+23s)} \end{aligned} \tag{37}$$

FIGURE 21. Photo of the sextuple water tank system.

TABLE 1. Controller parameters.

	Kp	Ti	Td
KC	1.50	54	14
SIMC	1.31	47	12
AMIGO	0.94	38	12

The tuning of the universal tuner has been done for specifications of gain margin GM = 2.5 and phase margin PM = 55. The controller parameters are given in Table 1.

The successful results and details of the slope calculation, signals used and controller derivation are described in [39].

C. ON IMPLEMENTATION ASPECTS

Notice the controllers presented here are of PID-type. The methods presented here for slope calculation with a single sine experiment on the process and the controller parameter optimization may be used for any structure of controller function, with the necessary adaptations. If PID-type control is used in practice, it is often necessary to add a filter to the derivative term. This may be used as part of the design as discussed in [40], [41], or it can simply be tuned such that the artificial pole has no influence on the dominant dynamics of the system. Altogether reducing its effect even for non-experienced users requires to divide the controller form by the extra pole.

From the testing point of view, a sinusoid is not a difficult test to perform on the real industrial process. In a manifold of real life processes, often the controlled output is in manual mode (which implies a certain degree of sluggishness) or in closed loop mode within a tolerance interval. Hence, the sine may be included with an amplitude to accommodate the tolerance interval during continuous operation.

The manner in which the slope and controller parameters are calculated allow for the method to be implemented in an autonomous mode, i.e. as an automatic tuner.

V. CONCLUSION

A direct controller tuning method is presented with inherent robust properties to measurement noise and process

disturbances. The proposed method has been extensively tested in simulation on a variety of processes representative for industrial applications and lower loop control problems. Extensive experimental validation has also been performed successfully. The controller type is PID-type, but the method is generically applicable to any controller structure. There are no known limitations of the proposed method. Although an important industrial control problem is ratio control, the method presented here has not yet been evaluated for this type of industrial control loop.

APPENDIX A

Property of the Laplace transform yields

$$\frac{dF(s)}{ds} = L\{-t \cdot f(t)\} \tag{38}$$

The signal $x(t)$ is the output of the process $P(s)$ to an input signal $t \cdot u(t)$. It follows that

$$X(s) = P(s)L\{t \cdot u(t)\} \tag{39}$$

with $X(s)$ the Laplace transform of the signal $x(t)$. Using the property of the Laplace transform it follows

$$X(s) = -P(s)\frac{dU(s)}{ds} \tag{40}$$

The Laplace transform of the signal $u(t)$ and its derivative are given by

$$\begin{aligned} U(s) &= \frac{A_u\bar{\omega}}{s^2+\bar{\omega}^2} \\ \frac{dU(s)}{ds} &= -\frac{2A_u\bar{\omega}s}{(s^2+\bar{\omega})^2} = -\frac{2s}{s^2+\bar{\omega}^2}U(s) \end{aligned} \tag{41}$$

Using (40) leads to

$$X(s) = -P(s)\frac{dU(s)}{ds} = \frac{2s}{s^2+\bar{\omega}^2}P(s)U(s) = \frac{2s}{s^2+\bar{\omega}^2}Y(s) \tag{42}$$

which suggests that the signal $x(t)$ may be obtained from the measured process output $y(t)$. The derivative of $Y(s) = P(s)U(s)$ is

$$\frac{dY(s)}{ds} = \frac{dP(s)}{ds}U(s) + P(s)\frac{dU(s)}{ds} \tag{43}$$

Recalling $\bar{Y}(s) = \frac{dP(s)}{ds}U(s)$ and (40) it follows that

$$\frac{dY(s)}{ds} = \bar{Y}(s) - X(s) \tag{44}$$

whose inverse Laplace is

$$-t * y(t) = \bar{y}(t) - x(t) \tag{45}$$

which completes the proof.

APPENDIX B

In order to provide support for algorithm implementation, an example from the paper is fully illustrated with corresponding programs and functions in Matlab. The users are kindly advised to cite this paper when using the software provided by the authors. The software can be found at the following location: Clara Ionescu - UGent (2019). Universal tuner for all types of processes (https://www.mathworks.com/matlabcentral/fileexchange/71759-universal-tuner-for-all-types-of-processes), MATLAB Central File Exchange. Retrieved June 5, 2019.

REFERENCES

[1] K. Starr, "Single loop control methods," ABB, Zürich, Switzerland, Tech. Rep., 2015.
[2] M. Skilton and F. Hovsepian, *The 4th Industrial Revolution*. Basingstoke, U.K.: Palgrave Macmillan, 2018.
[3] LCCC Workshop on Process Control, Department of Automatic Control. (2016). *Lund Center for Control of Complex Engineering Systems*. [Online]. Available: www.lccc.lth.se
[4] M. Bauer, A. Horch, L. Xie, M. Jelali, and N. Thornhill, "The current state of control loop performance monitoring—A survey of application in industry," *J. Process Control*, vol. 38, pp. 1–10, Feb. 2016. doi: 10.1016/j.jprocont.2015.11.002.
[5] ETFA. Accessed: Jun. 21, 2019. [Online]. Available: https://ieeexplore.ieee.org/xpl/conhome.jsp?punumber=1000260
[6] (Jun. 2018). *Report of This Event Was Published in the IFAC Electronic Newsletter*. [Online]. Available: https://www.ifac-control.org/
[7] A. Maxim, D. Copot, C. Copot, and C. M. Ionescu, "The 5W's for control as part of industry 4.0: Why, what, where, who, and when—A PID and MPC control perspective," *Inventions*, vol. 4, no. 1, p. 10, 2019. doi: 10.3390/inventions4010010.
[8] T. Liu, Q.-G. Wang, and H.-P. Huang, "A tutorial review on process identification from step or relay feedback test," *J. Process Control*, vol. 23, no. 10, pp. 1597–1623, 2013.
[9] T. Liu and F. Gao, *Industrial Process Identification and Control Design: Step-Test and Relay-Experiment-Based Methods* (Advances in Industrial Control). London, U.K.: Springer-Verlag, 2012.
[10] T. Samad, "A survey on industry impact and challenges thereof [technical activities]," *IEEE Control Syst. Mag.*, vol. 37, no. 1, pp. 17–18, Feb. 2017.
[11] J. Sánchez, M. Guinaldo, A. Visioli, and S. Dormido, "Identification of process transfer function parameters in event-based PI control loops," *ISA Trans.*, vol. 75, pp. 157–171, 2018.
[12] J. Sánchez, M. Guinaldo, A. Visioli, and S. Dormido, "Enhanced event-based identification procedure for process control," *Ind. Eng. Chem. Res.*, vol. 57, no. 21, pp. 7218–7231, 2018.
[13] L. Merigo, M. Beschi, F. Padula, and A. Visioli, "A noise-filtering event generator for PIDPlus controllers," *J. Franklin Inst.*, vol. 355, no. 2, pp. 774–802, 2018.
[14] K. J. Åström and T. Hägglund, *Advanced PID Control*. Fort Belvoir, VA, USA: ISA, 2006.
[15] C.-C. Yu, *Autotuning of PID Controllers: A Relay Feedback Approach*. London, U.K.: Springer-Verlag, 2006.
[16] M. Johnson and M. Moradi, *PID Control*. London, U.K.: Springer-Verlag, 2005.
[17] J. Berner, T. Hägglund, and K. J. AÅström, "Asymmetric relay autotuning—Practical features for industrial use," *Control Eng. Pract.*, vol. 54, pp. 231–245, Sep. 2016.
[18] K. Soltesz and A. Cervin, "When is PID a good choice?" in *Proc. IFAC-Conf. Adv. PID Control PID*, Ghent, Belgium, May 2018, pp. 250–255.
[19] Q. Bi, W.-J. Cai, E.-L. Lee, Q.-G. Wang, C.-C. Hang, and Y. Zhang, "Robust identification of first-order plus dead-time model from step response," *Control Eng. Pract.*, vol. 7, no. 1, pp. 71–77, 1999.
[20] V. Alfaro and R. Vilanova, "Model-reference robust tuning of PID controllers," in *Advances in Industrial Control*. Cham, Switzerland: Springer, 2016.
[21] D. Copot, M. Ghita, and C. M. Ionescu, "Simple alternatives to PID-type control for processes with variable time-delay," *Processes*, vol. 7, no. 3, 2019, Art. no. 143. doi: 10.3390/pr7030146.

[22] C. A. Monje, Y. Q. Chen, B. M. Vinagre, D. Xue, and V. Feliu, *Fractional-Order Systems and Controls* (Advances in Industrial Control Series). London, U.K.: Springer-Verlag, 2010.
[23] S. Skogestad and C. Grimholt, "The SIMC method for smooth PID controller tuning," in *PID Control in the Third Millennium* (Advances in Industrial Control), R. Vilanova and A. Visioli, Eds. London, U.K.: Springer-Verlag, 2012, ch. 5, pp. 147–175.
[24] J. Schoukens and R. Pintelon, *Frequency Domain Identification*. Piscataway, NJ, USA: IEEE Press, 2001.
[25] I. Boiko, "Non-parametric tuning of PID controllers," in *A Modified Relay-Feedback Test Approach* (Advances in Industrial Control). London, U.K.: Springer-Verlag, 2013.
[26] K. Papadopoulos, *PID Controller Tuning Using the Magnitude Optimum Criterion*. Cham, Switzerland: Springer, 2015.
[27] A. Roebel, "Frequency slope estimation and its application for non-stationary sinusoidal parameter estimation," in *Proc. 10th Int. Conf. Digit. Audio Effects (DAFx)*, Bordeaux, France, 2007, pp. 77–84.
[28] A. Karimi, D. Garcia, and R. Longchamp, "PID controller tuning using Bode's integrals," *IEEE Trans. Control Syst. Technol.*, vol. 11, no. 6, pp. 812–821, Nov. 2003.
[29] F. Padula and A. Visioli, *Advances in Robust Fractional Control*. Cham, Switzerland: Springer, 2015.
[30] I. Birs, C. Muresan, I. Nascu, and C. Ionescu, "A survey of recent advances in fractional order control for time delay systems," *IEEE Access*, vol. 7, pp. 30951–30965, 2019. doi: 10.1109/ACCESS.2019.2902567.
[31] R. De Keyser, C. I. Muresan, and C. M. Ionescu, "A novel auto-tuning method for fractional order PI/PD controllers," *ISA Trans.*, vol. 62, pp. 268–275, May 2016.
[32] R. De Keyser, A. Dutta, A. Hernandez, and C. M. Ionescu, "A specifications based PID autotuner," in *Proc. IEEE Int. Conf. Control Appl.*, Dubrovnik, Croatia, Oct. 2012, pp. 1621–1626.
[33] R. De Keyser, C. M. Ionescu, and C. I. Muresan, "Comparative evaluation of a novel principle for PID autotuning," in *Proc. 11th Asian Control Conf. (ASCC)*, Gold Coast, QLD, Australia, Dec. 2017, pp. 1164–1169. doi: 10.1109/ASCC.2017.8287335.
[34] C. Copot, C. Muresan, C.-M. Ionescu, S. Vanlanduit, and R. De Keyser, "Calibration of UR10 robot controller through simple auto-tuning approach," *Robot.*, vol. 7, no. 3, p. 35, 2018. doi: 10.3390/robotics7030035.
[35] C. I. Muresan, C. Copot, I. Birs, R. De Keyser, S. Vanlanduit, and C. M. Ionescu, "Experimental validation of a novel auto-tuning method for a fractional order PI controller on an UR10 robot," *Algorithms*, vol. 11, no. 7, p. 95, 2018. doi: 10.3390/a11070095.
[36] C. I. Muresan, R. De Keyser, I. R. Birs, S. Folea, and O. Prodan, "An auto-tuning method for a fractional order PD controller for vibration suppression," in *Proc. Int. Workshop Math. Methods Eng. (MME)*, Ankara, Turkey, 2018, pp. 245–256.
[37] R. De Keyser, C. I. Muresan, and C. M. Ionescu, "Autotuning of a robust fractional order PID controller," in *Proc. 9th IFAC Symp. Robust Control Design (ROCOND)*, Florianópolis, Brazilia, Sep. 2018, vol. 51, no. 25, pp. 466–471. doi: 10.1016/j.ifacol.2018.11.181.
[38] C. I. Muresan, R. De Keyser, I. R. Birs, D. Copot, and C.-M. Ionescu, "Benchmark challenge: A robust fractional order control autotuner for the refrigeration systems based on vapor compression," in *Proc. 3rd IFAC Conf. Adv. Proportional-Integral-Derivative Control (PID)*, 2018, vol. 51, no. 4, pp. 31–36. doi: 10.1016/j.ifacol.2018.06.021.
[39] R. De Keyser and C. I. Muresan, "Validation of the KC autotuning principle on a multi-tank pilot process," in *Proc. IFAC Symp. Dyn. Control Process Syst., Including Biosyst. (DYCOPS)*, Florianópolis, Brazil, Apr. 2019, pp. 178–183.
[40] A. Leva and M. Maggio, "Extending ideal PID tuning rules to the ISA real structure: Two procedures and a benchmark campaign," *Ind. Eng. Chem. Res.*, vol. 50, no. 16, pp. 9657–9666, 2011.
[41] A. Visioli, *Practical PID Control* (Advances in Industrial Control). London, U.K.: Springer-Verlag, 2006.

ROBIN DE KEYSER received the M.Sc. degree in electromechanical engineering and the Ph.D. degree in control engineering from Ghent University, Gent, Belgium, in 1974 and 1980, respectively, where he is currently an Emeritus Senior Professor of control engineering with the Faculty of Engineering and Architecture. His research interests include model-predictive control, auto-tuning and adaptive control, modeling and simulation, and system identification.

CRISTINA I. MURESAN received the Ph.D. degree in advanced control of nuclear processes from the Technical University of Cluj-Napoca, Romania, in 2011, where she is currently an Associate Professor. Her research interests include control of various processes, dead-time compensation, and fractional-order control.

CLARA M. IONESCU received the Ph.D. degree in (bio-)science engineering from Ghent University, Belgium, in 2009, where she has been a tenure-track Professor, since 2016. Since 2012, she has been a Researcher with the Technical University of Cluj-Napoca, Romania. Her research interest includes modeling and control of dynamical processes, with special focus on process control and biomedical processes. She was a grant holder of the Prestigious Fellowship Award from the Flanders Research Centre, from 2011 to 2017.